

Pyrotron Plasma-Heating Experiments

By F. H. Coengen, F. C. Ford and R. E. Ellis*

R. F. Post¹ has proposed that an ionized gas (plasma) can possibly be contained in a linear magnetic field of circular symmetry. The motion of charged particles along the magnetic field lines is to be limited by strong magnetic fields (magnetic mirrors) at the ends of the system. (See Curve A, Figure 1.) He has discussed the properties of a plasma in such a magnetic field configuration from the premise that an individual charged particle of a tenuous plasma will behave as an isolated ion in a magnetic field. If one also assumes that the gradient of the magnetic field (∇B) is small over a region of the order of an ion orbit and that the time rate of change of the magnetic field (dB/dt) is so slow that the magnetic field is essentially constant for the time of one ion rotation, the motion of an ion conforms with the following relations:

$$\text{magnetic moment} = \mu = W/B = \text{constant} \quad (1)$$

$$\text{and} \quad \oint P_z dz = \text{constant}. \quad (2)$$

The axis of symmetry of the magnetic field is taken as the z coordinate. For convenience, the symbols used in this paper are defined as follows:

W = the rotational energy of an ion associated with the component of velocity perpendicular to the magnetic field.

U = the translation energy of an ion associated with the component of velocity parallel to the magnetic field.

v = ion velocity.

θ = angle between the magnetic field vector and the ion velocity vector.

$v_{\perp} = v \sin \theta$ = component of velocity perpendicular to the magnetic field.

$v_{\parallel} = v \cos \theta$ = component of velocity parallel to the magnetic field.

m = ion mass.

$P_z = mv_{\parallel}$ = component of momentum parallel to magnetic field.

$R = B_m/B_c$, the instantaneous ratio of the maximum value to the minimum value of the magnetic field. Typically, B_c is located midway between two mirrors of value B_m .

$\alpha = B_t/B_0$, the ratio of the magnetic field at time t

to magnetic field at the same spacial point at time $t = 0$. In general, α is a function of position even for simple systems.

n = the number of electrons per cm^3 = the number of ions per cm^3 . Electric charge neutrality is assumed at all points in the plasma.

k = Boltzmann's Constant.

T = Temperature in degrees Kelvin.

$\beta = \frac{nkT}{B^2/8\pi}$, the ratio of particle energy density to magnetic field energy density.

L = distance between turning points of an ion, approximately equal to the separation of the magnetic mirrors.

$\gamma = L_t/L_0$, ratio between turning points of an ion at time t and time $t = 0$.

r = radius of plasma column.

ρ = radius of curvature of a charged particle in a magnetic field.

As the field changes slowly its value can be considered constant during the time necessary for the ion to move a distance L . Therefore, the total energy of the ions will not change during this interval, i.e.,

$$W + U = \frac{1}{2}mv^2 = \text{constant}. \quad (3)$$

From (1) and (3) it follows that the angle between the velocity vector of an ion and the magnetic field has the following dependence:

$$\frac{\sin \theta_c}{\sqrt{B_c}} = \frac{\sin \theta_z}{\sqrt{B_z}}, \quad (4)$$

where the subscript c denotes values taken at the field minimum, which is usually the center of a simple system. At the position for which $\sin \theta_z$ is unity, the velocity of the ion along the field line is zero. Here the ion stops and its motion along the field lines is reversed, that is, the ion is reflected. This behavior is the basis upon which plasma confinement by magnetic fields has been postulated. The condition for ion containment is then

$$\sin \theta_c \geq R^{-\frac{1}{2}}. \quad (5)$$

If an ion that initially has a rotational energy W_1 in a magnetic field B_1 is later found in a magnetic field B_2 , it follows from Eq. (1) that it will have an energy

$$W_2 = W_1(B_2/B_1). \quad (6)$$

From Eq. (2), if the distance between turning points

* University of California Radiation Laboratory, Livermore, California.

of a confined ion be changed from L_1 to L_2 , the translational energy will be given by

$$U_2 = U_1(L_1/L_2)^2. \quad (7)$$

Again, from the constancy of the magnetic moment it follows that

$$B\rho^2 = \text{constant}. \quad (8)$$

This, in turn, implies that the radius of the plasma in a magnetic field varies as

$$r_2 = r_1(B_1/B_2)^{1/2}. \quad (9)$$

By use of Eqs. (1) and (2) the density is found to be

$$n_2 = n_1(B_2/B_1)(L_1/L_2). \quad (10)$$

For $L_1 = L_2$ and $B_2 > B_1$ the density is seen to increase. Thus, if the magnetic field throughout a containment region is increased at every point with the same functional dependence, the density is increased, the ion energies are increased and the radius of the plasma column is decreased. Hence the simple operation in which the magnetic field is increased as a function of time is frequently referred to as a radial magnetic compression.

Similarly, an operation which decreases the longitudinal extent of the plasma is referred to as a longitudinal compression. A longitudinal compression can be performed without increasing B in the central part of the system. Therefore, β can be increased.

$$\beta_2 = \beta_1(L_1/L_2). \quad (11)$$

β is constant for a radial compression.

HISTORICAL DEVELOPMENT OF THE HIGH COMPRESSION EXPERIMENTS

It was first proposed that a plasma be established in a magnetic field of mirror geometry by injecting a beam of energetic ions into an initially evacuated chamber. The ion beam was to be trapped by increasing the magnetic field. Since the density of neutral particles was low, the loss of energetic ions by charge exchange would be low. The loss rate due to scattering could be reduced by use of high energy ions because the Coulomb cross section is inversely proportional to the square of the ion energy. System I (see Table 1) was designed to use a beam of 5-kv ions. However, a suitable source had not been developed at the time the vacuum and coil systems were completed in February 1954. Therefore, the experiment was performed using the plasma generated by an electric arc of 10- μ sec duration between deuterium-loaded titanium electrodes. The delay between initiating the pulsed magnetic field and striking the arc was varied from zero to a few hundred microseconds. A microwave interferometer² was used to determine the electron density and study its decay. Densities of the order of 10^{12} electrons per cubic centimeter were found. The characteristic decay time was typically 500 μ sec. These observations were the first experimental evidence of a plasma magnetically heated and confined. Although

accurate determinations of the energy distributions for the ions and electrons were not made, it is known from the time-of-flight measurements that the mean ion energy did not exceed 5 ev, before compression.

Table 1. Comparison of Systems I, II and III

	I	II	III
Internal diameter of vacuum chamber at the center	6"	2"	6"
Distance between dc mirrors	no dc	24"	76"
Distance between pulsed magnetic field mirrors	44"	6"	32"
Pulsed field mirror ratio .	2 : 1	2 : 1	1.5 : 1
Pulsed field rise time .	500 μ sec	50 μ sec	500 μ sec
Pulsed field decay time .	10 msec	3 msec	30 msec
Capacitor bank energy .	2×10^5 joules	3.2×10^6 joules	10^6 joules
Approximate peak magnetic field at mirror .	3×10^4 gauss	11.4×10^4 gauss	4.4×10^4 gauss

In fabricating System I it was necessary to develop magnet coils of exceptional strength for the high magnetic fields. Continued improvement of the magnet coils made it possible to utilize pulsed magnetic fields up to 2×10^5 gauss. Thus it appeared possible to produce a plasma with a mean ion energy of a few kilovolts by use of magnetic compression (see Eq. (6)), if the low-energy plasma could be confined in a weak magnetic field.

System II was built specifically to achieve a large value for the ratio of the final magnetic field to initial magnetic field, that is, a high magnetic compression. Radiation from this system was first detected by scintillation counters external to the vacuum and coil systems late in January 1955. The investigation was interrupted at that time to allow the experiments to be moved to larger quarters. However, by July 1955 it was determined that the radiation was primarily x-rays in the energy range from 10 kev to 200 kev. When the 6-inch system was rebuilt in the new laboratory it was provided with dc field coils, System III.

The signal variations from one operation to the next were found to be much smaller for System III than for System II. Therefore, all the detailed investigations have been made in the former system.

DESCRIPTION OF SYSTEM III

The main vacuum chamber is a Pyrex glass pipe of 6-inch internal diameter. A thin stainless-steel coating is evaporated on the inner surface, to assure that all points of the vacuum chamber walls will be at the same potential. A base pressure of 2×10^{-7} mm Hg is achieved with a 6-inch mercury diffusion pump. End ports are provided through which plasma sources and detection equipment can be introduced.

Two sets of magnetic field coils surround the vacuum chamber and are coaxial with it (see Fig. 1). A dc current is passed through the large coil set to provide

a dc magnetic field up to 400 gauss in the mirror regions (Curve A, Fig. 1). Current is supplied to the coils of small diameter by a 1.2 millifarad capacitor bank which can be charged to 40 kv. The pulsed coil and the capacitor bank form essentially a large series circuit of an inductance, a resistance, and a capacitance, as shown in Fig. 2. Each series switch (S_1) is a group of four 5555-type mercury ignitrons. The series resistance in the circuit is small so that current rise is nearly sinusoidal (see Curve A, Fig. 2). At the time the current in the coil is a maximum, switch S_2 is closed. The current then decays with a time constant equal to the inductance of the short circuit loop divided by the resistance of this loop. S_2 is made up of eight 5555-type ignitrons arranged in four parallel paths.

In a typical operation the plasma is injected into the dc magnetic field about 20 μ sec before the pulsed magnetic field is applied. The field reaches its maximum value in approximately 500 μ sec and decays to $1/e$ of its maximum value in 30 milliseconds.

OBSERVATIONS AND DISCUSSION

Density Studies

After the source is fired a charged particle density of 10^{10} to 10^{13} electrons/cm³ is observed in the central region of the system. The density decays to $1/e$ of its maximum value in times from 50 μ sec to a few hundred μ sec. The decay time is found to depend upon

the initial density, the magnetic field configuration, details of the plasma source and the orientation of the source. If the source is fired into a uniform magnetic field there is no observable containment of the plasma.

The ions trapped in the dc field must satisfy the condition for reflection (Eq. (5)) and miss the source upon returning to the point of injection. Those ions that collide in the initially dense plasma in the vicinity of the source will return to the point of collision rather than to the source.

As the microwave interferometer will not follow rapidly changing densities or accurately detect the density of small plasma columns, it has been impossible to determine the density as a function of time after applying the pulsed field. Langmuir-type probe studies of a plasma in a weak magnetic field agree with the microwave data.

Plasma Compression

As discussed above, the product of the magnetic field and the square of the radius of the plasma column should remain constant for a purely radial compression. If the magnetic field is given by $B_t = B_1 + B_m \sin \omega t$, the radius of the plasma column as a function of time should be

$$r_t = r_1 [1 + (B_m/B_1) \sin \omega t]^{1/2}, \tag{12}$$

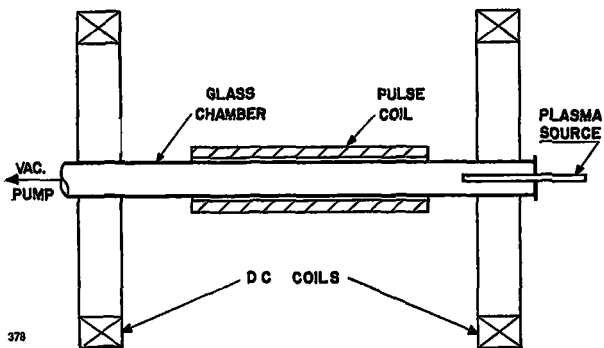
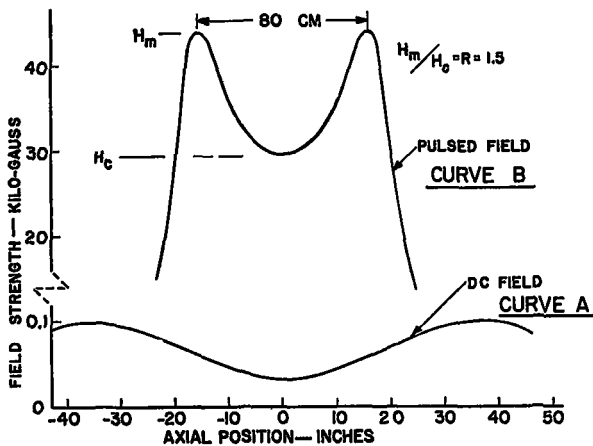


Figure 1. Schematic diagram and magnetic field distributions for System III

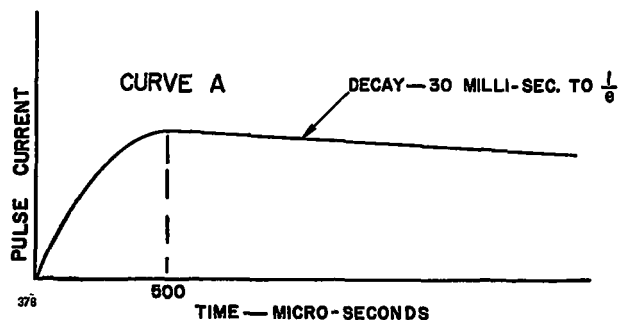
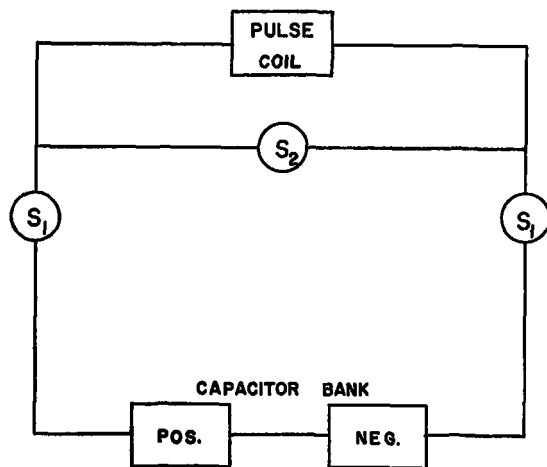


Figure 2. Pulse coil circuit and time dependence of the current in the pulsed coil for System III

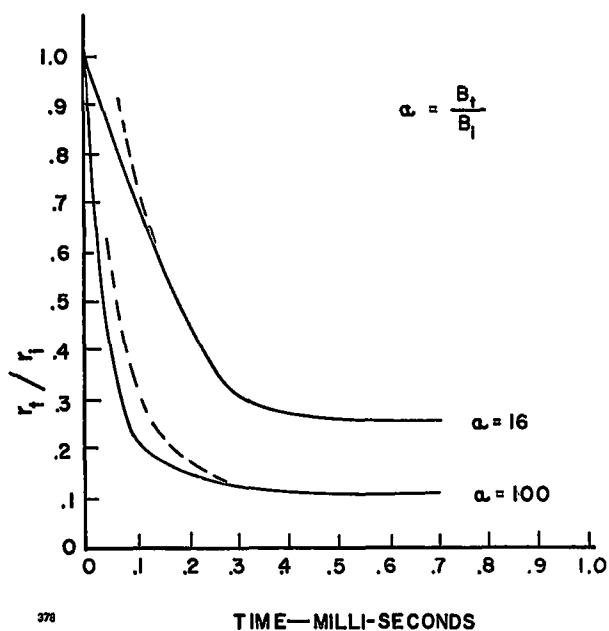


Figure 3. Radial positions of the surface of the plasma column as a function of time for the plasma in System III. The solid curves are plotted from Eq. (12) and the dashed curves from probe measurements

where r_1 is the initial radius of the plasma. A small probe, whose radial position could be varied, was inserted at the midplane of the pulsed coil system. The probe signals were found to drop suddenly to zero at a time t after the pulsed magnetic field was applied. If t is taken as the time the plasma boundary passed the probe position one obtains a curve as shown in Fig. 3. The discrepancy between the experimental curve and that predicted by Eq. (12) could be due in part to the fact that the plasma which is compressed by a mirror field is also expected to be longitudinally compressed. Thus the individual charged particles gain more energy than in a simple radial compression.

Another set of observations that demonstrate the compression of the plasma column was taken with a small NaI scintillation crystal and a photomultiplier. The crystal was shielded so that X-rays could enter only the front surface. Relative X-ray intensities were then observed outside of the vacuum chamber walls as a function of longitudinal position. Previous investigations have shown that all but a small part of the X-rays are generated at the walls. Thus if it is assumed that the energy distribution of the electrons striking each part of the walls is the same, and that the electrons which strike a portion of the wall traveled along magnetic field lines from the interior of the compressed plasma, the radial distribution of the plasma can be inferred from the measured X-ray signals (see Fig. 4).

Attempts have been made to study the electron energy distribution by introducing electron sensitive emulsions into the vacuum system and locating them at one mirror. It is necessary to coat the emulsions in order to exclude light; consequently, low-energy electrons are excluded from the emulsion. However, the

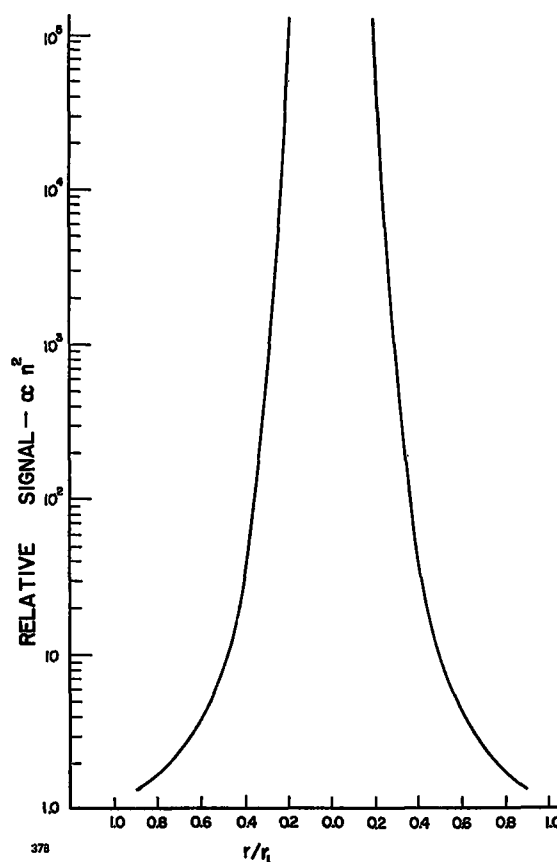


Figure 4. Plasma distribution in System III as deduced from the z-dependence of the X-ray signals

high-energy electrons are concentrated in a cylinder no larger than $\frac{3}{8}$ inch at the mirror.

Heating

To date there is evidence only for electron heating, as techniques for ion measurements are still in the developmental stage.

The earliest evidence for considerable heating of some of the electrons was, of course, the energetic X-rays. Later, as discussed by C. B. Wharton,² microwave noise measurements were made using a 25 kilomegacycle narrow band width system. This technique gives a "noise temperature" between 10 and 20 kev. Some information of the electron energy distribution is obtained from the emulsions. Again, large numbers of electrons with energies up to 50 kev are observed. It should be pointed out that none of these techniques will detect the low-energy electrons of the initial electron energy distribution. R. E. Ellis (of this Laboratory) has carried out the most careful study of the electron energy distribution and he discusses the method and results in the following paragraphs.

ELECTRON ENERGY DISTRIBUTION

Using a scintillator detector, measurements of the signal produced by electrons escaping through the loss cone of one of the mirrors of System III have been made to obtain information concerning the energy

distribution of the escaping electrons. Consideration of the processes by means of which particles leak through the mirrors permits these energy distribution measurements to be referred to the plasma inside the mirrors, and the relative numbers of electrons per unit energy interval at a given energy may be determined as a function of time.

Method

The data discussed here were obtained by placing a scintillator detector at a position approximately on the magnetic axis of the machine and 3 inches outside the mirror at the end opposite the source. Particles escaping through the loss cone, along the magnetic axis of the machine, passed through thin aluminum and aluminum-coated plastic absorber foils and were collimated by a $\frac{1}{8}$ -inch hole in the stainless steel probe head before entering the detector. The scintillator, of the terphenyl-loaded styrene plastic type, was vapor-coated with 2000 Å of Al for light-tightness. The signal produced in a photomultiplier tube with cathode follower was displayed on an oscilloscope and photographed.

The runs were made by taking 5 to 10 pulses for a given absorber value and capacitor-bank voltage. Figure 5 shows the experimental points obtained for a peak magnetic field of ~ 32 kilogauss, with 20 μ sec delay between source firing and initiation of the field pulse, and an elapsed time of $\tau = 1$ millisecond after the source was fired (peak magnetic field occurs at $\sim 600 \mu$ sec).

In addition to the signal from the electron scintillator probe, the signals from two NaI scintillator detectors were used as monitors in a limited sense. One NaI detector viewed the X-rays emerging from the side of the machine at a position midway between the mirrors, and the other was arranged so as to view the X-rays emerging from one end of the machine, more or less axially. Since there appeared to be no consistent correlation between the magnitude of the X-ray pulses and the electron probe pulse, it was not possible to use these detectors as quantitative monitors. Long-term monitoring of machine stability was accomplished by taking zero absorber runs at given machine parameters. Statistical averaging was used to normalize from pulse to pulse.

Analysis of Data

The statistical reliability of the raw data is about 50%, based on the number of pulses taken for each absorber value. In order to analyze the data at the present state of the experiment it has been assumed that (1) the loss of electrons to the detector caused by collision diffusion in the absorber foils may be neglected, and (2) the relative scintillation efficiency of the plastic detector for electrons is essentially the same as that of anthracene crystal.³ An experiment has been designed, but not completed, to test the first assumption.

If we let the quantity $Q(E_0)$ represent the height of the oscilloscope pulse at a time τ subsequent to firing

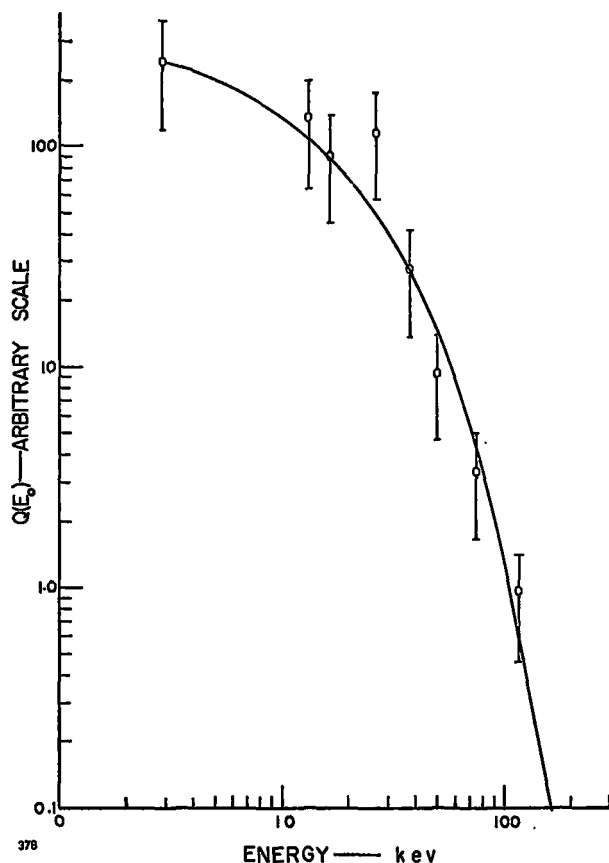


Figure 5. Probe signal $Q(E_0)$ vs. absorber thickness, E_0 , measured at time $\tau = 1$ millisecond subsequent to initiation of magnetic field pulse, 20- μ sec field delay, and ~ 32 -kilogauss peak pulse field

of the source, then, under our assumptions, $Q(E_0)$ is proportional to the light emitted by the scintillator, in a small time-interval centered about τ , due to the flux of electrons which have passed through the absorber (of thickness equivalent to E_0) and stopped in the scintillator. Then for the j th absorber, of thickness E_{0j} , we have

$$Q_j(E_{0j}) = K \int_{E_{0j}}^{\infty} n(E)g(E, E_{0j})\epsilon(g)dE. \quad (13)$$

Here K is a constant relating to the parameters of the detection system and $n(E)$ is the number of electrons per unit energy interval, at energy E , in the flux of electrons which has diffused through the mirror along the magnetic axis of the machine. The function $g(E, E_{0j})$ represents the energy given up to the fluor by an electron of energy E . The percentage of the energy transferred to the fluor (by an electron) which is converted into emitted light is represented by the scintillation efficiency ϵ and is a function of g , the energy which an electron has when it enters the fluor.

Equation (13) may also be written as

$$Q_j(E_{0j}) = K \int_{E_{0j}}^{\infty} n(E)F(E, E_{0j})dE, \quad (14)$$

where $F(E, E_{0j}) = g(E, E_{0j})\epsilon(g)$. Now $g(E, E_{0j})$ may

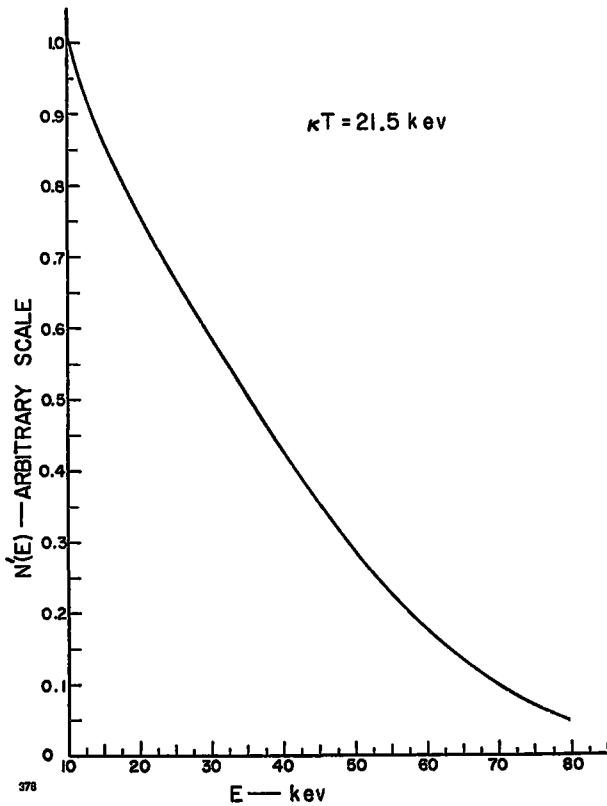


Figure 6. Relative electron energy distribution $N'(E)$ vs. E in kev for plasma electrons for $\kappa T = 21.5$ kev, based on data in Fig. 5

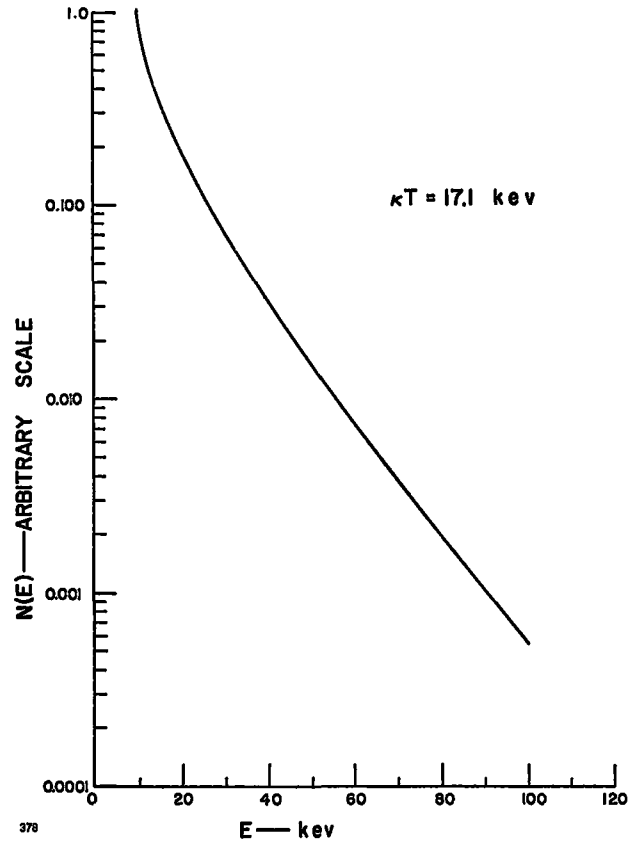


Figure 7. Relative electron energy distribution $N(E)$ vs. E in kev for escaping electrons for $\kappa T = 17.1$ kev, based on data in Fig. 5

be computed from energy-range curves for electrons in aluminum^{4, 5} and $\epsilon(g)$ taken from the empirical curve for anthracene.³

The solution of Eq. (14) may be written as

$$\begin{aligned}
 Q_j(E_{0j}) &\approx K \int_{E_{0j}}^{100 \text{ kev}} n(E) F(E, E_{0j}) dE \\
 &\quad + \frac{\gamma}{(\kappa T)^{3/2}} \int_{100 \text{ kev}}^{325 \text{ kev}} E^{1/2} e^{-E/\kappa T} F(E, E_{0j}) dE \\
 &\approx K \sum_{m=0}^j F_{mj}(E_m, E_{0j}) n_m(E_m) + R_j(E_{0j}).
 \end{aligned} \quad (15)$$

Here we have assumed that above 100 kev the distribution will be essentially a three-dimensional Maxwellian and that the contribution, to the signal, of electrons above 325 kev in energy will be negligible. The contribution to the signal from electrons with $E > 100$ kev is represented by $R_j(E_{0j})$. The contribution from electrons with energy $E \leq 100$ kev is given by the discrete sum over $j+1$ intervals, where $K F_{mj} n_m$ represents the contribution of electrons of energy $E_m = E_{0j} + (j - m + \frac{1}{2}) \Delta E$; $\Delta E = 10$ kev. The constant γ results from the Maxwellian normalization factor and the detector parameters and κT is the kinetic temperature of the electrons in kev. The quantity $(n_0 E_0)$ represents the number of electrons per kev at an average energy $E_0 = 100$ kev in the

energy interval 95 kev to 105 kev; $n_1(E_1)$ represents the number of electrons at $E_1 = 90$ kev in the interval from 85 kev to 95 kev, etc.; F_{mj} represents the light emitted for electrons of energy E_m when absorber E_{0j} is in place. The quantities $K n_j$ may be solved for explicitly and the relative distribution $N(E)$ obtained when the R_j have been evaluated. The constant γ may be evaluated on the assumption of a high-energy Maxwellian tail for the distribution by taking the ratio of $Q_m(E_{0m})$ to $Q_n(E_{0n})$ for two energies and finding by trial substitution the value of κT that satisfies the equation for the ratio of these two experimental quantities.

Interpretation

To relate this analysis to the plasma electrons, we substitute for $n(E)$ in Eq. (14) a distribution modified by Coulomb scattering of electrons by plasma ions so that Eq. (14) becomes

$$Q_j(E_{0j}) = K' \int_{E_{0j}}^{\infty} E^{-3/2} n'(E) F(E, E_{0j}) dE, \quad (16)$$

where the primed quantities are those changed by the scattering process. The value of κT obtained for the plasma electrons on the basis of the smooth curve shown in Fig. 5 is $\kappa T = 21.5$ kev, using $Q(65 \text{ kev})/Q(95 \text{ kev})$. With other equally probable smooth curves

drawn through the experimental points in Fig. 5, a range of κT values from 21 to 27 keV is obtained. Using the value of $\kappa T = 21.5$ keV and a three-dimensional Maxwellian distribution for $n(E)$ in Eq. (16), the values obtained for Q (15 keV) and Q (35 keV) are 94% and 102%, respectively, of the experimental quantities derived from the smooth curve in Fig. 5. The relative distribution $N'(E)$ based on the smooth curve in Fig. 5 is shown in Fig. 6.

Using the unmodified distribution, $n(E)$, the relative distribution for the escaping electrons is shown in Fig. 7. A value of $\kappa T = 17.1$ keV was obtained for the escaping electrons, using the same data.

The fractional error in the results for the temperature of the plasma electrons is at least of the same order of magnitude as for the experimental quantities, i.e., $\sim 50\%$. More precise data and more extensive investigation of the type of trial distribution used to compute the value of Eq. (16) should lead to a more dependable estimate of the plasma temperature. The smooth distributions obtained result from the use of a smooth curve through the data points. Even though the R_j are computed independently, they are relatively small and vary by about a factor of 2.5 between 5 and 95 keV. The n_j have large absolute errors in this analysis and the use of an iterative technique for their determination may be advantageous.

CONCLUSIONS

The experiments to date have shown that a plasma can be compressed by a pulsed magnetic field and that the plasma column moves as predicted. There is a large amount of evidence for electron heating. However, it has not been shown that the heating follows the adiabatic law (Eq. (6)).

Since the X-ray and electron signals persist for times of the order of 30 milliseconds, containment of a plasma is indicated. Furthermore, the lack of discontinuities or "bursts" in the X-ray and electron signals suggests that the plasma is stable. However, better information of the plasma density, energy content and composition are needed before significant statements can be made concerning containment or stability. If the total energy that is measured by a scintillator or a thermocouple located at one mirror is integrated, it is found that the particle energy density in the confinement volume at the end of the compression was of the order of 8% of the magnetic field energy density. Further work is in progress to improve the accuracy of the measurement.

Many modifications of the single-stage compression experiment can be made. Radial injection of the initial plasma at the midplane is a simple variation that has recently been introduced. Preliminary operation indicates that the radial injection utilizes the plasma source more effectively, resulting in higher final particle energies in the plasma.

REFERENCES

1. R. F. Post, *General Theory of Pyrotrons*, Unpublished Report.
2. C. C. Damm, J. C. Howard and C. B. Wharton, *Plasma Diagnostic Developments in the UCRL Pyrotron Program*, Paper P/381, Vol. 32, these Proceedings.
3. O. R. Frisch, *Progress in Nuclear Physics*, Pergamon Press, New York, Vol. 5, Chap. 7 (1956).
4. Ann T. Nelms, *Energy Loss and Range of Electrons and Positrons*, National Bureau of Standards Circular, 577 (July 26, 1956).
5. L. Katz and A. S. Penfold, *Phys. Rev.*, **24**, 28 (1952).